

THREE YEARS OF OPERATION OF THE ONERA PRESSURIZED SUBSONIC WIND TUNNEL

by Jean-Marie CARRARA and Alain MASSON

Office National d'Etudes et de Recherches Aéropatiales, 92320 Châtillon, France

SUMMARY

Three years after the entry into service of the pressurized subsonic wind tunnel F1 of ONERA, at Le Fauga-Mauzac, a first survey of its utilization and operation can be presented.

After a brief description of the wind tunnel and its instrumentation, the paper recalls its aerodynamic characteristics and performance. The operational domain is larger than the contractual : thus, the 4 bar maximum pressure can be used up to 80 m/s instead of the expected 70 m/s.

The various testing devices of the wind tunnel are described, and some original testing techniques are presented. The variety of the tests performed since entry into service is illustrated by a few typical examples.

The results are a proof of the interest of this facility for the study of the respective effects of Mach and Reynolds numbers ; a comparison with flight results of those obtained on a model of Mercure makes it possible to globally validate the quality of the wind tunnel.

1. INTRODUCTION

The F1 wind tunnel, installed by ONERA on the site of the new Fauga-Mauzac Centre, some 30 km south of Toulouse (fig. 1), is operational since 1977 (first running on 10 August, first tests on models in November).

The increase of wind loadings and the reduction of runway lengths required by transport aircraft make mandatory an ever more detailed research on high lift devices on the wings for manoeuvres close to the ground (take off and landing). Also, manoeuvrability at high angle of attack of combat aircraft calls upon a widespread experimentation in a range where air viscosity effects must be correctly simulated [1].

The F1 wind tunnel, pressurized up to 4 bar, which makes it possible to reach during tests on models significant Reynolds numbers and to study the effects of a variation of this parameter, independtly of variations of Mach number, meets the needs of the study of present-day aircraft at low speeds.

Furthermore, this wind tunnel has been designed with a view to reduce as far as possible the duration of the tests and to offer the greatest flexibility in their sequence. Besides tests of industrial type, it also offers broad possibilities for performing tests of a research character aimed at the fine study and the development of mathematical models of flows.

The final adjustment of the F1 wind tunnel and its exploitation have been conducted, since its entry into service, with a view to the best possible adaptation to these various types of problems.

A very important effort, still to be pursued, has been done to provide the F1 wind tunnel with very high performance testing equipment, care being taken to ensure its compatibility with other large European wind tunnels, particularly S1-MA[2], the 5-m RAE and the DNW wind tunnels.

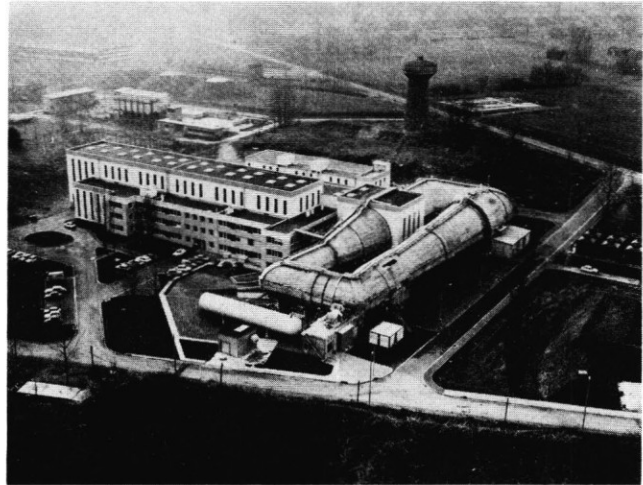


Fig. 1 - The pressurized subsonic wind tunnel F1 of the Fauga-Mauzac Centre.

2. GENERAL CHARACTERISTICS OF THE WIND TUNNEL [3]

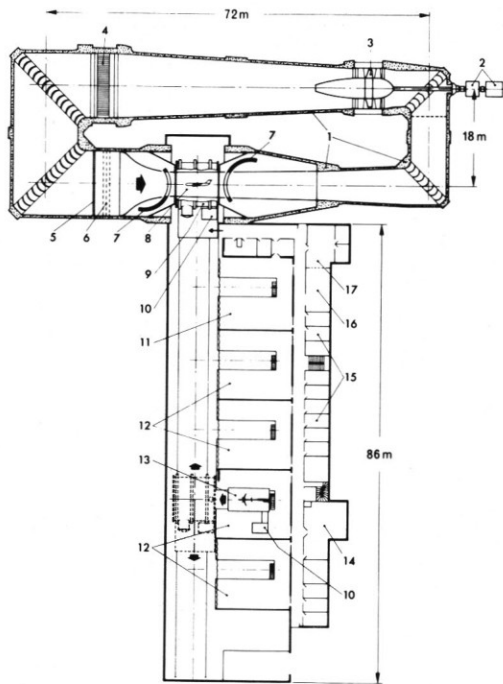
This wind tunnel is original as regards its design and the technology used for its construction :

- its design allows a fast testing rate ; the solutions retained appear as well adapted operationally ;

- its structure is made of prestressed concrete, a technology chosen in view of very marked gains on delay and cost of construction.

2.1 Aerodynamic circuit (fig. 2)

The F1 wind tunnel is of pressurized, closed circuit type. The rectangular circuit, 72 x 18 m between axes, has an overall volume of some 13 000 m<sup>3</sup>. A part corresponding to the test section, of a volume limited to 450 m<sup>3</sup>, can be pneumatically isolated, and depressurized independently of the rest of the circuit, which permits rapid handlings on the test mounting. The settling chamber is 12 m in diameter. A metallic convergent ensures the passage to the rectangular test section, with a 7.2 contraction ratio.



1. Pre-stressed concrete aerodynamic circuit
2. Driving assembly
3. Variable pitch fan
4. Cooler
5. Aerodynamic filter
6. Anti-turbulence screens
7. Isolating doors
8. Test section (with a floor-mounted half-model)
9. Trolley
10. Measuring unit
11. Cell with load application bench
12. Test preparation cells
13. Interchangeable model-carrier
14. Workshop
15. Offices for constructor's representatives
16. Data processing room
17. Test control room

Fig. 2 - Plan of aerodynamic circuit and exploitation building.

A first diffuser, also metallic, ensures the gradual return to a circular cross section ; its mean aperture angle is  $5^\circ$ . The first corner is 6.8 m in diameter. The part between corners 1 and 2 is cylindrical ; it includes an inclined net for catching any element accidentally torn from the test mounting. The air intake for the wind tunnel pressurization is also in this part.

The driving fan is located behind corner 2 ; further downstream, a second conical diffuser, of  $6^\circ$  aperture angle, ensures the link with this last part, a 12-m-dia. cylinder. Just before corner 3, a cooling apparatus, made of a battery of water tubes with flanges, evacuates the energy dissipated in the wind tunnel.

Behind corner 4, the settling chamber is preceded by a honeycomb filter (depth 200 mm, 25 mm side hexagonal meshing) and three anti-turbulence grids (1 mm dia. metallic wires, 4 mm side square meshing).

## 2.2 Testing trolley and carts

In the test section part, the circuit leaves room for a mobile assembly : the testing trolley. The continuity of efforts of the concrete part is ensured by two beams, above and under the trolley

berth. This 8 m long assembly runs on rails all along the exploitation building. It contains the central part of the test section (this extends on either side in the circuit, and have an effective overall length of 11m, of rectangular cross section (3.5 m in height, 4.5 m in width). The two vertical walls and the roof are solid with the trolley ; the floor itself is detachable, and constitutes a cart carrying the testing apparatus, the model and the data acquisition unit. Three interchangeable carts equip the wind tunnel at present.

Figure 3 schematizes the operation of this assembly. The carts are in the position of test preparation, each in one of the five cells of the exploitation building. The trolley is brought in front of a cell when a test is considered as ready (all checkings without wind having already been performed). The cart is introduced into the trolley (movement 1), then the trolley is driven to the test position, ensuring the continuity of the aerodynamic circuit. (movement 2).

Upstream and downstream of the trolley, two cylindrical doors, with vertical axis, close the circuit, which enables one to have access to the trolley, and even to remove it while the rest of the wind tunnel is still under pressure.

A system of inflatable joints ensure the airtightness of all junctions.

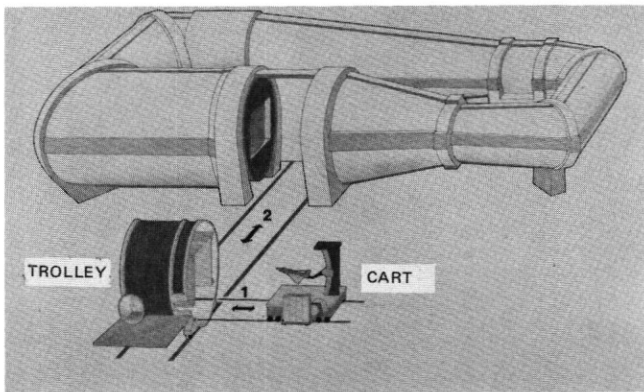


Fig. 3 - Schematics of the operation of testing trolley and carts.

## 2.3 Cells

Five cells permit the preparation of the tests outside the wind tunnel test section. They are separated from one another, which makes it possible to preserve the confidential character of the tests (the general architecture of the wind tunnel is adapted to meet this important requirement).

A wide room is offered around the cart, with a view to make easy staff and hardware displacements. Offices close to these cells are at the disposal of the clients staff.

Handling devices are available for the preparation of tests : a 250 kN gantry and a 20 kN rolling beam.

## 2.4 Wind tunnel drive

The wind tunnel motor is a 9500 kW asynchronous electric motor supplied under 5500 volts, located outside the pressurized circuit. It is followed by a speed reducer driving the fan through a shaft crossing the airtight structure and the corner n° 2.

The fan rotates at a constant speed (360 r.p.m.) it is made of 16 blades with variable pitch (rotor) ; it is followed by a 17 fixed blade stator ensuring an axial flow. The bulb covering the hub is 3.8 m in diameter ; it is held by 14 supporting struts upstream and 3 downstream. The external diameter of the fan is 7.4m.

The pitch of the 16 mobile blades is piloted by an electro-hydraulic servocontrol which, for an assigned velocity  $V$ , ensures a velocity stability better than  $10^{-3}V$  above  $V = 50$  m/s.

## 2.5 Compressed air plant

The compressed air generation is obtained by a 4-stage centrifugal compressor providing a 6 kg/s flowrate under an outlet pressure of 11 bar. The wind tunnel is supplied through a 300 m<sup>3</sup> buffer tank that can be used for regulating the pressure around an assigned value. A servocontrol ensures the stability of the stagnation pressure with a dispersion lower than  $\pm 1.10^{-3}$ .

The machines building and the circuits are planned to allow a second compressor driven by an identical motor, and to complement this installation with a high pressure compressor and appropriate storage.

## 2.6 Cooling apparatus

A water cooler made of flanged tubes, and the associated air-cooling device, make it possible to stabilize the stagnation temperature around an assigned value, between atmospheric temperature and 40°C. A servocontrol maintains this temperature around the assigned value within better than 1°C.

## 2.7 Wind tunnel control

Setting of the fan blades, compressed air supply system (adjusting valves at inlet and outlet) and adjustment of the cooling apparatus constitute the control parameters of the wind tunnel. Each can be actuated manually or by a servo-mechanism.

All the information is gathered in the wind tunnel control room. The operator responsible for the wind tunnel operation can, from this room, control the wind tunnel by direct manual controls or by addressing assigned values to the various servocontrols, through a MITRA 15 minicomputer calculating the assigned values of the three control parameters necessary for obtaining the desired testing conditions.

Further to this "regulation" function, the computer assumes monitoring tasks, edits the operation journal ("operator guide" function), and may ensure a sequential control of some devices in the wind tunnel ("automaton" function").

## 2.8 Measuring units (fig. 4)

Each cart possesses its own digital acquisition unit, mechanically attached to the mounting. The passage from the cell position (preparation and checking) to the wind tunnel position (actual test) does not entail any disconnection at low level, which makes it possible to validate the cell checkings and reduces the time of access to the test section. The objective is to start acquisition within the half hour following the start from the cell.

Each acquisition unit comprises a set of 64 analogue measuring channels, with signal conditioning and amplification, and filtering. These channels are scanned under the conduct of a computer (HP 2100 with 64 k-bytes memory and 5 M-bytes magnetic disc), which ensures :

- the measurement acquisitions,
- the metrologic checking of the analogue part,
- the on-line monitoring of the test,
- the digital control of the model support,
- the transmission of data to the control computer.

Processing is ensured by the central computer (IRIS 80), which returns the results during the tests ; this computer possesses :

- a central memory with 192 k-words of 32 bits (768 k-bytes),
- four units of removable discs of a capacity close to 400 M-bytes,
- four unwinders for 9-channels 1600 b.p.i. tapes.

On this computer, a system specific to the ONERA test centres [4,5] has been developed with a view to take into account several simultaneous tests (e.g. checking measurements in a cell and actual tunnel test). Also, the writing of processing programmes is made easier by an original system of aid to programming.

## 2.9 Test running

When the model is in the wind tunnel test section, the set of parameters necessary for conducting and monitoring the test is gathered in the "test control room". The dialogues with the HP 2100 (local) and IRIS 80 (central) computers are ensured by a cathode screen console for each. The display of the results, in the form desired by the test engineer is immediately obtained in this room :

- on the cathode console, with hard copy,
- on fast printer,
- on curve plotter.

A number of parameters, chosen by the test engineer, are permanently displayed on digital receivers.

An elaborate television set permits the permanent visualization of the model and of the vital parts of the wind tunnel (net, fan, etc.).

## 3. AERODYNAMIC CHARACTERISTICS AND PERFORMANCE

The pressure distributions over the circuit made it possible, on the one hand, to ascertain the pressure losses and the performance of the wind tunnel and, on the other hand, to characterize the flow quality.

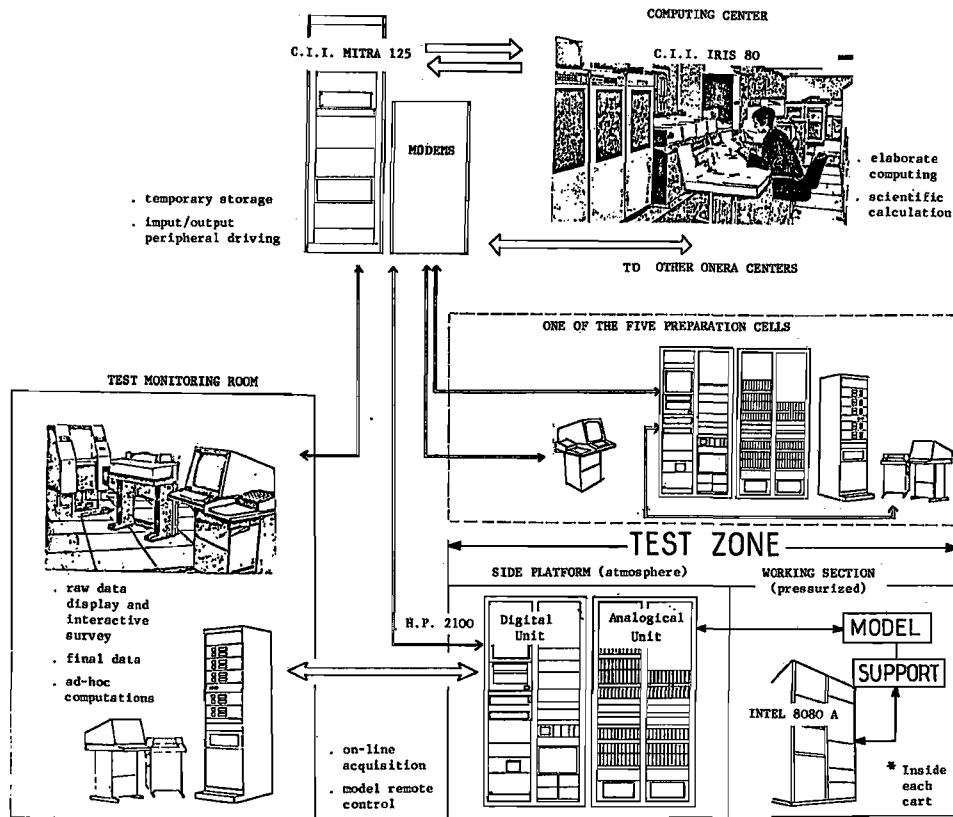


Fig. 4 - Synoptic table of data acquisition.

### 3.1 Pressure losses and performance (fig. 5)

The large number of measurements in various locations of the wind tunnel made it possible to ascertain the pressure drops in the main elements of the circuit.

The pressure drops, as indicated, are the quotient of  $\Delta p$  (difference of the weighted mean stagnation pressures between the upstream and the downstream cross sections of the element considered) by the kinetic pressure in the test section,  $q$ . The actual pressure drops are most often lower than expected.

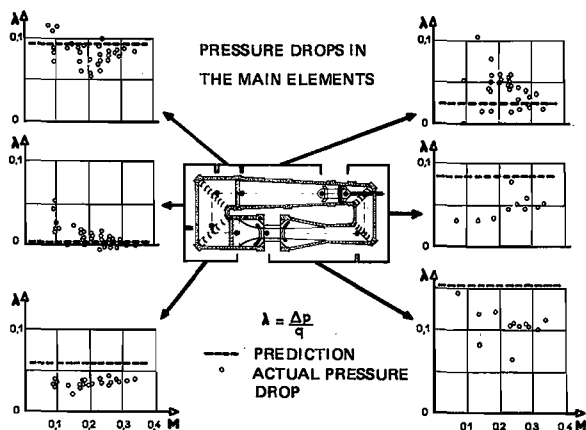


Fig. 5 - Pressure loss of various elements of the circuit.

Figure 6 shows the evolution of the overall pressure loss in the wind tunnel in the four following cases : 1) test section empty, 2) with sting holding sector, 3) with sting holding sector carrying a 1-m-dia. disc perpendicular to the wind and simulating the pressure drop of a model and 4) with a parachute in the first diffuser of the wind tunnel, also simulating a strong pressure drop. We shall remark the effect of the increase of Mach number and of the increase of stagnation pressure  $p_0$  on the decrease of pressure drop. With sting holding sector, the overall pressure drop is between 0.36 and 0.31 at atmospheric pressure, but lower by about 0.04 at 3.9 bar.

The predictions had retained the maximum value of 0.42 without model, and 0.49 for a very large model with flow separation.

Thus, there appears a reserve of power at the limits of the contractual operation domain. This domain is presented on figure 7 as Mach number versus Reynolds number (conventionally calculated with one tenth of the square root of the test section, viz. 0.397 m for F1).

Considering this available power reserve, complementary tests have been undertaken in 1979, in cooperation with the fan constructor (Turbo Luft-Technik, GmbH) to widen the testing domain of the wind tunnel.

The fan blades have been equipped with strain gages, the current measuring installation of the wind tunnel has been complemented with unsteady pressure transducers, and steps have been taken

STAGNATION PRESSURE

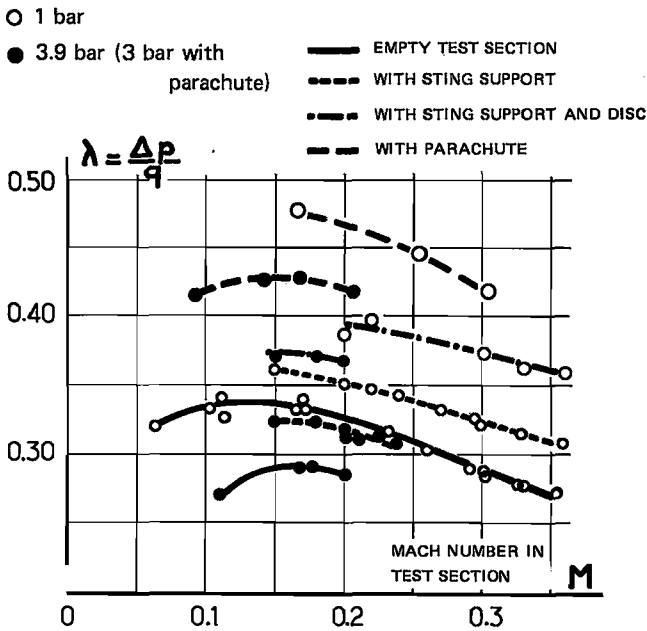


Fig. 6 - Evolution of the overall pressure loss of the wind tunnel.

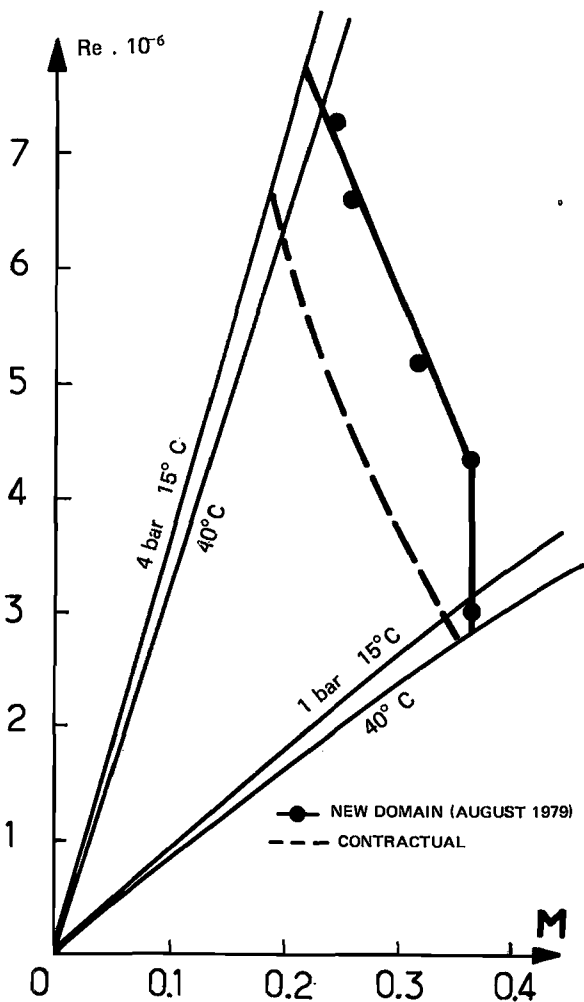


Fig. 7 - Testing domain of the wind tunnel.

to check during the tests the behaviour of some elements (cooler, honeycombs, net, etc.) whose mechanical strength is difficult to ascertain a priori.

Checking points have first been performed within the previously explored domain, with two pressure drop configurations : sting holder equipped or not with the 1 m dia. disc. The extended domain has then been explored with the sting holder alone, up to a maximum kinetic pressure of 14 000 pascals, instead of 11 000 as before.

Figure 7 locates the extreme points investigated. In these conditions, the maximum power reached never exceeded 8500 kW (for a 9500 kW nominal power of the motor), so that the power reserve is sufficient to cover the new domain with the usual models tested.

3.2 Aerodynamic characteristics

Figure 8 presents the distribution of stagnation pressure in various sections of the wind tunnel. The flanged tube cooler, giving a high pressure drop, supplies a homogeneous flow to the settling chamber ; this effect is complemented by the honeycomb filter and the three grids.

In the test section, a slight divergence of the two vertical walls compensates the variation of the boundary layer thickness along the test section, so as to ensure a flow without longitudinal gradient. The boundary layer thickness (at 99%) varies from 60 to 150 mm from the beginning to the end of the test section.

The flow is checked by the simultaneous measurement of static pressures on the roof and the right lateral wall, and on a probe located on the section axis with great precision, in the presence of the sting holder downstream of the test section.

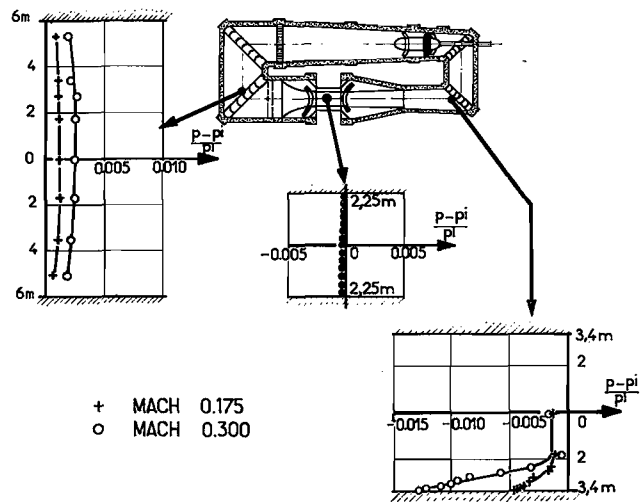


Fig. 8 - Distribution of characteristic pressures in the circuit.

Figure 9 makes it possible to verify the absence of longitudinal gradient within the volume occupied by the model.

The survey of the pressure distribution on the walls during tests of a large model shows

that the reference pick-up, a Prandtl antenna, placed in the upstream part of the test section, is not influenced by the presence of the model (fig. 9).

The flow angularity in the test section is zero, with an inaccuracy of  $\pm 0.02$  degree.

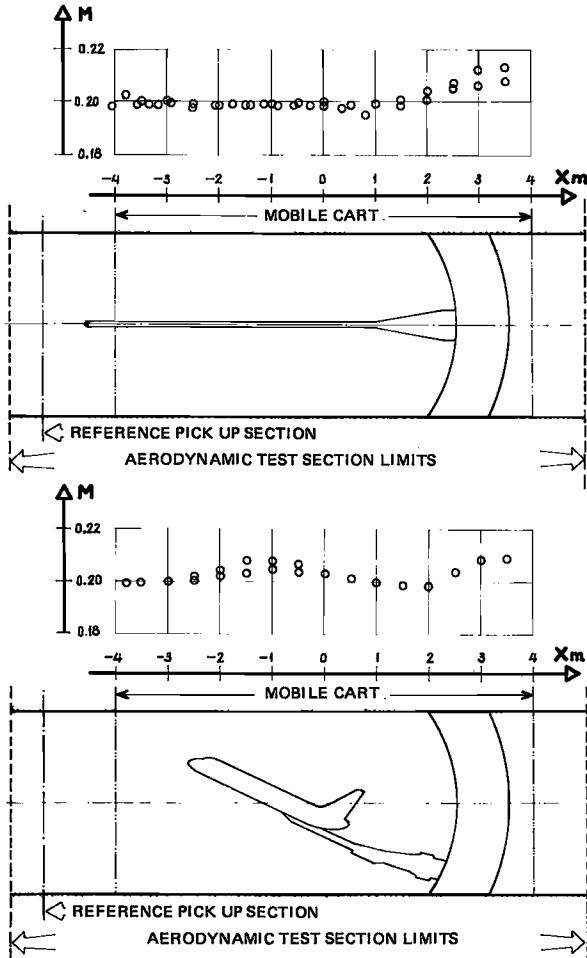


Fig. 9 – Static pressure in the test section.

A crosswise exploration of stagnation pressure in the middle of the test section verified the perfect uniformity of the flow (fig. 10).

$p_i$ (Pa) \ M	0,10	0,20	0,30	0,35
100 000	10	20	50	70
200 000	20	40	50	
300 000	30	60		
380 000	40	80		

Each value, in Pa, is the maximal difference between stagnation pressure measured along transversal rake (length 4,5 m) and the reference stagnation pressure.

Fig. 10 – Stagnation pressure in the test section.

The first measurements concerning the unsteady characteristics of the flow<sup>[3]</sup>, performed with various instruments (hot wires, microphones, unsteady pressure transducers) show (fig. 11) a very low level of turbulence, lower than 0.01%, and a satisfactory noise level within the velocity range most frequently used in the wind tunnel.

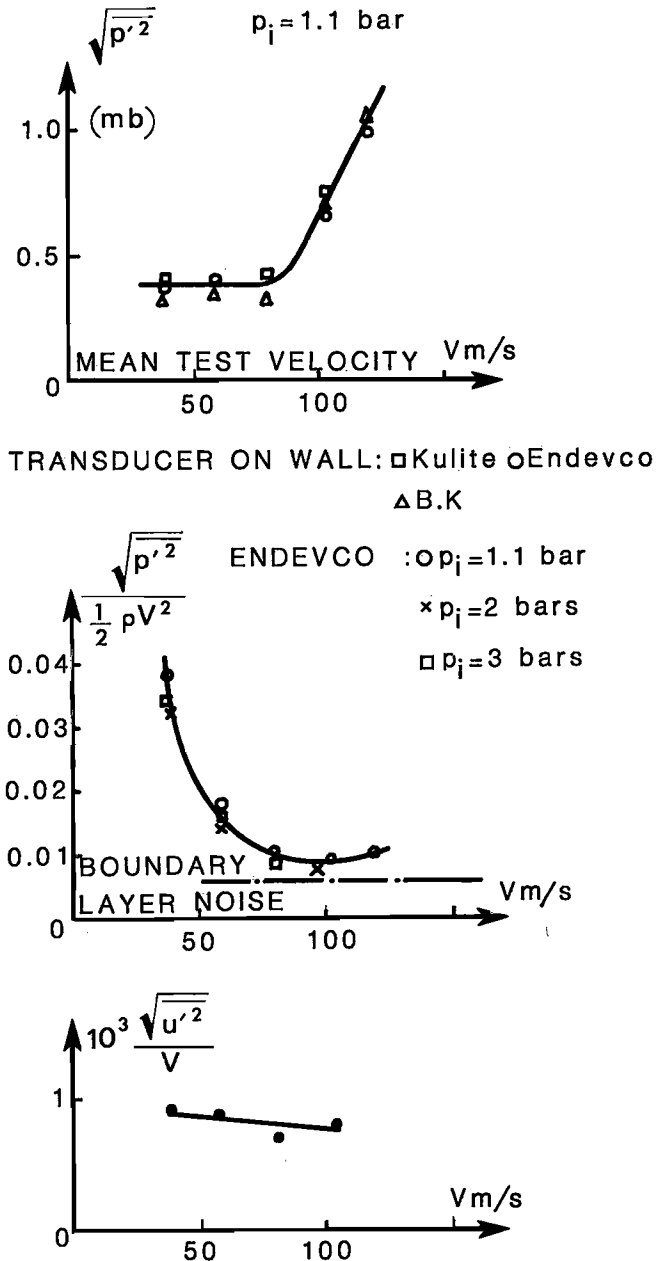


Fig. 11 – Noise and turbulence in the test section.

Spectral analyses of the signals did not reveal any peculiarity at very high frequency. Complementary tests are undertaken to globally confirm the low-turbulence character of the flow, and to look for the origin of the spectral tones between 0 and 1000 Hz, e.g. the appearance of a noise at 690 Hz above 90 m/s.

The results already acquired are not yet sufficiently conclusive, and this work will be pursued.

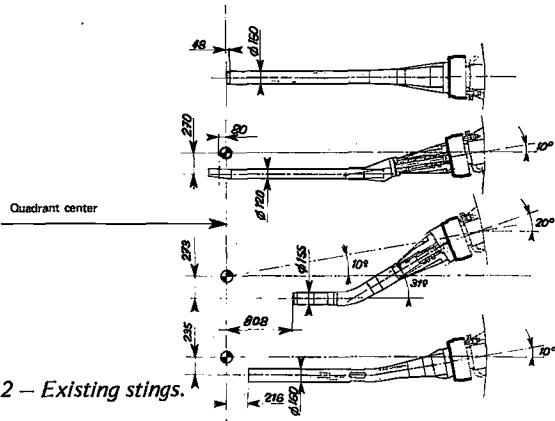


Fig. 12 - Existing stings.

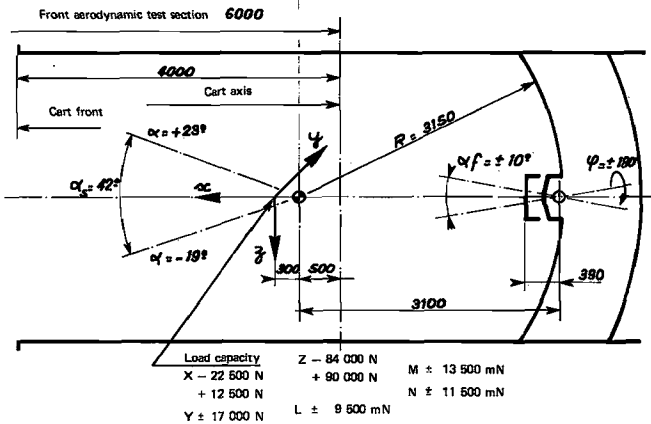


Fig. 13 - Sting holding sector.

An evaluation of the critical Reynolds number on a sphere verifies the small turbulence level of F1 : the result is comprised between 330.000 and 380.000 in the wind tunnel range.

#### 4. THE TESTING DEVICES

Three carts are at present available. One of them, carries a sting holder ; the other two are intended for other types of mountings.

##### 4.1 Cart n° 1 - Sting holding support

Figure 13 recalls the main characteristics of the sting holder quadrant of F1.

A jointed coupling of the stings on the quadrant maintains at the test section centre the model even through it is in front of the sector centre of rotation. The use of bent stings allows all the pitch angles desired for the tests, the exploration range being 42°.

The various motorized rotations of the sting holder sector are carried out at adjustable rates, up to 1°/s. A digital control, built around a microcomputer, ensures the conduct of the whole assembly with assigned values (angular positions and displacement rate) defined in digital form.

This control can be directly addressed by the computer in charge of acquisition.

On this mounting, many series of tests have already been carried out on models of AMD/BA

aircraft : Mercure (1/10 scale) and Mirage 2000 (1/4.28 scale). The available stings are represented on figure 12.

##### 4.2 Carts n° 2 and 3

Both these carts are equipped with a turn table supporting the various mountings : for half models at the wall, of complete models on vertical strut or on three struts. Figure 14 gives the maximum capacities of this device.

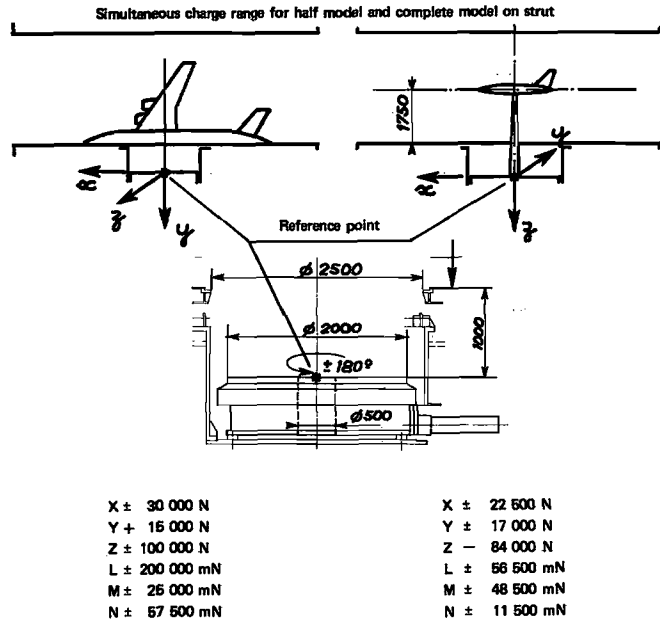


Fig. 14 - Wall turntables of carts no 2 and 3.

Among the possible mountings, represented on figure 15, one should remark that mountings n° 1 and 2 make use of a balance of the S1-MA wind tunnel of the Modane Centre, although successfully used at F1 for tests of half models of the wall, they are usually replaced by mounting n° 3. This mounting will use a new wall balance (fig. 16), which will be equipped with a dual sensitivity drag dynamometer.

In the same manner, mountings n° 4 and 5 will usually be replaced by mounting n° 6, also called "Xtable".

However, the choice between one or the other of these 6 mountings will always be possible, according to the desired characteristics of the tests.

A classical 3-strut mounting, which will be fixed on the upper wall of the wall balance, is at present under study, and will be available for tests programmed in 1981.

So, for a civil aircraft, the four types of mounting represented on figure 17 will be possible, and will allow useful comparisons : mounting on sting holder, by straight or bent sting, mounting on vertical strut, 3-strut mounting.

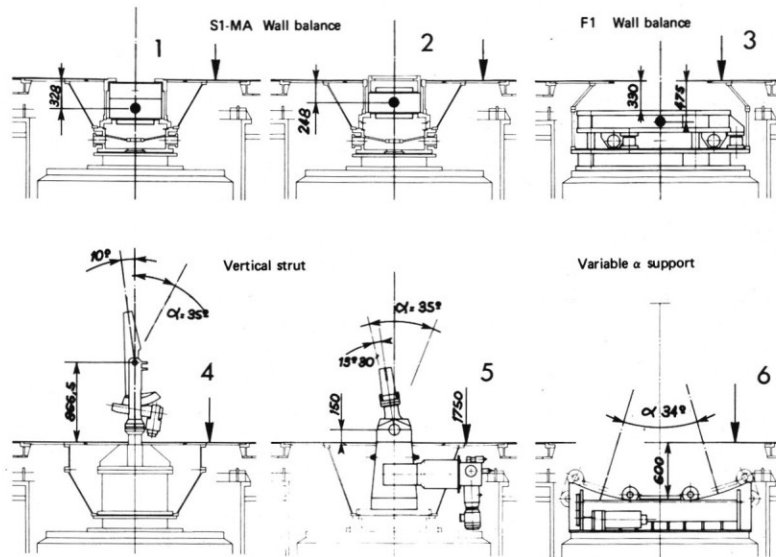


Fig. 15 - Various mountings on wall turntable.



Fig. 16 - Wall balance of F1.

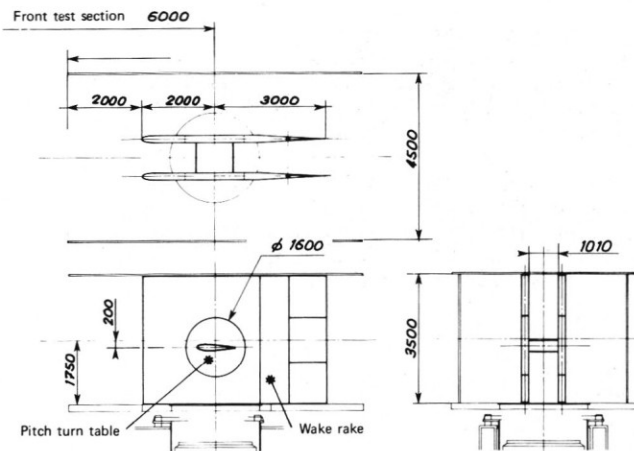


Fig. 18 - The two-dimensional test section of F1.

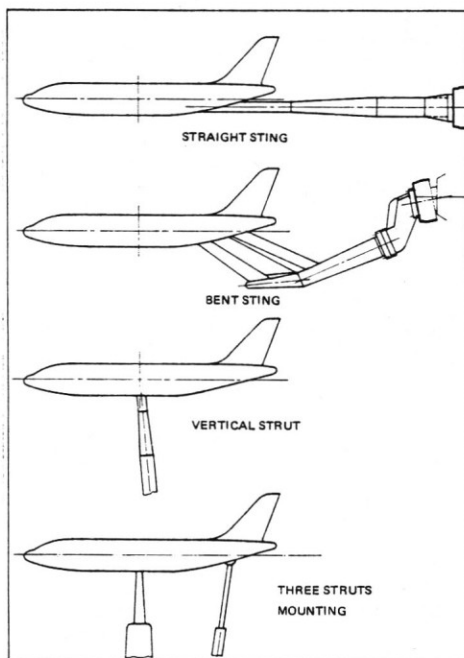


Fig. 17 - Various mountings of a civil aircraft.

#### 4.3 Two-dimensional mounting (fig. 18)

For tests on wing profiles, the choice has been made of a test section of reduced span, of width 1.01 or 1.50 m, obtained between two large vertical flanges. The test mounting is identical to that previously used in the former ONERA wind tunnel of Cannes. The solution retained allows tests on relatively small models, easier to fabricate and to implement. The counterpart is that one has to better master the problems of interaction with the lateral flanges : this is obtained by boundary layer suction.

Each flange is equipped with trailing edge flaps, whose adjustment makes it possible to control the circulation around the flange, and thus to obtain a test section free from longitudinal pressure gradient. Classical measurements are used for the measurement of global efforts on the profiles : integration of wall pressures on the model for lift, wake exploration for drag.

A mobile rake makes it possible to explore the field close to the profile, along local normals ; the measurements performed are of several types : stagnation pressures, velocities and Reynolds shear stress by hot wires.



#### 4.4 Mounting for large scale air intakes

The wind tunnel has been equipped in December 1979 for air intake tests at large Reynolds numbers. Models at 1/4 scale allow studies, at the same Reynolds number as in flight, problems related to the air intake functioning at low speed, at take-off or landing, as the wind tunnel is pressurized at 4 bar.

The tank made up by the pressurized circuit of the wind tunnel is used to supply to flowrate through the air intake, ensured by the communication with the atmosphere through a system of flowmeters and valves, along the principle shown on figure 19.

The main circuit, of about 50 kg/s flowrate and comprizing two pre-adjustment valves, opens up into the exhaust silencer of the wind tunnel, capable of a 60 kg/s flow rate ; a complementary circuit can extend the flowrate to 75 kg/s, the adjustment of this complementary flowrate being obtained by a fixed, interchangeable throat.

The opening of the two shutting valves initiates the flow through the air intake model. The flow-rate measurement is ensured by means of Venturis, whose calibration has been performed during preliminary tests by means of sonic throat nozzles.

The dimensions of the installation permit a maximum flowrate of 75 kg/s at 4 bar, quite sufficient for testing 1/4 scale models of combat aircraft air intake. A slightly smaller scale must be chosen for models of air intakes of Airbus type aircraft.

The model can be placed facing the wind, on a mounting with universal joint allowing pitch and yaw adjustments, within a wide range. The influence of cross wind at very low or zero speed (case of sideslip reaching 90°) is studied by mounting vertically in the test section, on the exhaust duct, the assembly made of the air intake and its jointed support.

The same assembly might be installed in the S1 wind tunnel of Modane for the study of the air intake in high subsonic flow, up to Mach numbers close to 1.

#### 5. EXAMPLES OF PARTICULAR TESTS AND TESTING TECHNIQUES

During three years of use of the wind tunnel, shared between technological and aerodynamic adjustments, industrial tests and research tests, a harvest of results has already been obtained, among which let us mention :

- civil aircraft : tests on a complete 1/10 scale model of Mercure 100, tests on a 1/16 scale half model of Airbus A310;
- military aircraft : tests on a complete 1/4.28 scale model of Mirage 2000, tests in a 1/2.5 half model of Alphajet.
- research tests on a variable sweep wing, with and without canard ;
- development of methods for studying the near field of the flow around military aircraft (applicable to civil aircraft) : device for exploring the pressure field, visualization by laser plane and smokes ;

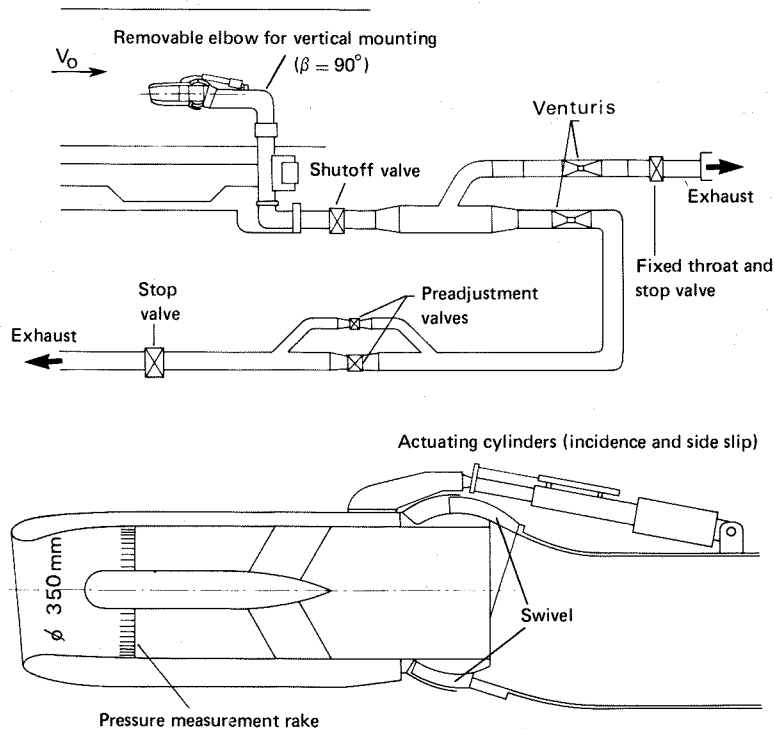


Fig. 19 - Mounting for testing large scale air intakes.

- tests of dynamic stability of military aircraft ;
- tests of missiles at high angle of attack ;
- tests of parachutes ;
- two-dimensional tests on profiles : conventional profile, thick profile, blown profile, with conventional measurements and detailed exploration of the field ;
- tests of a General Electric air intake for Airbus A310 at 1/6.25 scale, of an Aérospatiale air intake for Airbus A200 at 1/5 scale.

The rythm of these works led to the performance of about twenty different tests during the year 1979.

### 5.1 Mercure 100

The 1/10 scale model of Mercure 100, which had been constructed in cruise configuration for tests at S1-MA, was well adapted for qualification tests of F1 in view of its dimensions (3-m-span) and of the possibility it offered to make comparisons between the results of F1 and S1-MA, in the same conditions for the same model, and comparisons with exploitations of test flights carried out by the AMD/BA Company.

For tests at F1, a wing equipped with high lift devices has been realized by the constructor (fig. 20).

The tests were performed on the model mounted on a sting supported by the wind tunnel sector, up to incidences varying, according to the configuration, from 12 to 25°.

A preliminary test had shown that the model was outside the aerodynamic field of the support.

The agreement between results, corrected for wall effect interference, obtained in cruise configuration at atmospheric pressure at F1 and S1-MA, is quite satisfactory (fig. 21) : the curves  $C_L(\alpha)$

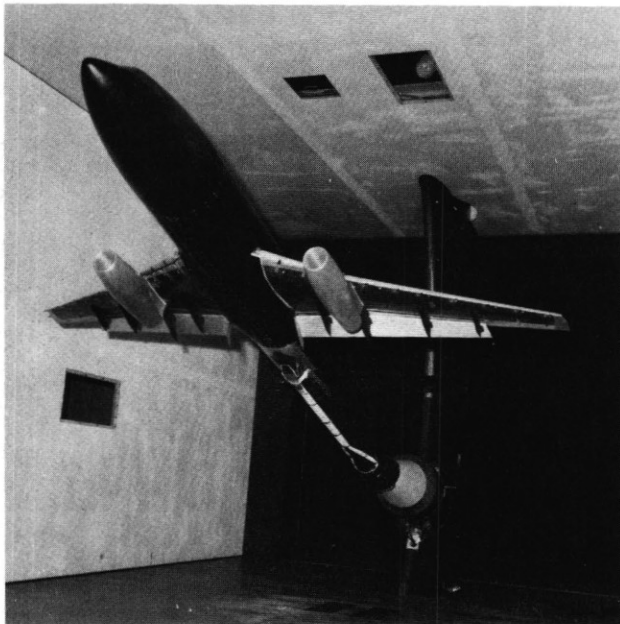


Fig. 20 - Mercure 100, landing configuration.

are identical, the polars  $C_L(C_D)$  and the stability curves  $C_L(C_m)$  are very similar. Thus this test validates the wall effect corrections of F1, which obviously are much larger than those of S1-MA, whose cross section is much larger.

The trimmed polars obtained at a stagnation pressure of 3.9 bar are compared on figure 22 with the results of the modelling made by AMD/BA and corresponding to flight results. The wind tunnel data are rough results, corrected for wall effects ; detectors placed on the high lift devices revealed that their displacements remained very small during the tests, even at high pressure.

The comparison can be made quite directly for the cruise and take-off configurations, for which the flight and wind tunnel tests concern undercarriage-up configurations. The flight results at landing correspond to the undercarriage down, while all wind tunnel tests were made without undercarriage. It is however still possible to verify the good coherence of the flight and wind tunnel curves thanks to results in flight, at take-off, showing the influence of the undercarriage.

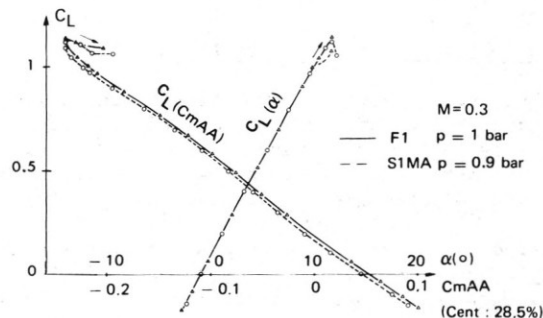
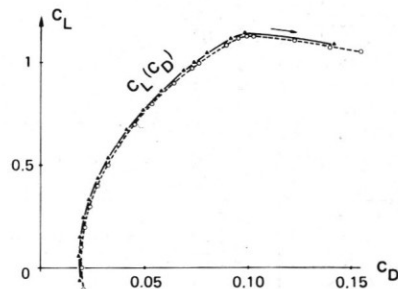


Fig. 21 - Mercure 100 (1/10 scale). Comparison between F1 and S1-MA.

The comparison of maximum lift coefficients reached in flight and in the wind tunnel is given in figure 23. On Mercure, the effect of the Reynolds number is very small, at least on the maximum lift coefficients with high lift devices on. The representation of the aircraft in the wind tunnel is quite correct.

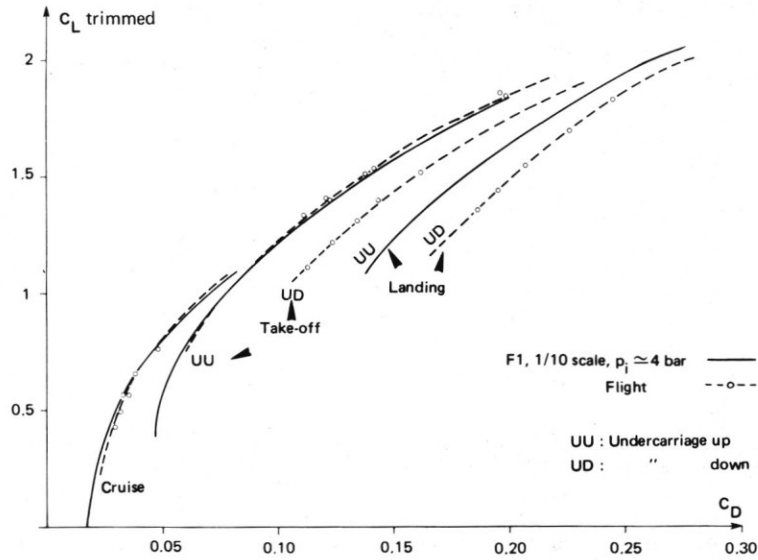


Fig. 22 – Mercure 100. Comparison between flight and F1 wind tunnel.

F1 Wind tunnel				C <sub>L</sub> max. Flight	
Configuration	M	Re 10 <sup>6</sup>	C <sub>z</sub> Maxi		
Cruise	0.15	1.6	1.07	2.08 (M = 0.2 Re = 15 · 10 <sup>6</sup> )	
	0.15	5.4	1.23		
	0.20	2.0	1.11		
	0.20	7.1	1.17		
Take-off	0.15	1.6	1.95		
	0.15	5.4	2.10		
	0.20	2.0	2.00		
Landing	0.15	1.6	2.50		2.50 (M = 0.17 Re = 13 · 10 <sup>6</sup> )
	0.15	5.4	2.55		
	0.20	2.0	2.50		
	0.20	7.1	2.55		

Fig. 23 – Comparison of maximum lift coefficients in flight and in the wind tunnel.

atmospheric wind tunnel, in which the Reynolds number variation is obtained by a variation of velocity.

### 5.3 Military aircraft

Figures 25 and 26 present a sting mounted, 1/4.28 scale model of Mirage 2000, and a 1/2.5 scale half model of Alphajet mounted at the wall. For both these tests, the wind tunnel reproduces the flight conditions (Mach and Reynolds). During Mirage 2000 tests the pitch angle reached 35° (for 3.85 bars and 70 m/s : 32°).

### 5.2 Half model of civil aircraft

Figure 24 shows the evolution of the maximum lift coefficient of a half model at 1/16 scale of an Airbus A310 when we vary either the Mach number (of constant Reynolds) or the Reynolds number (by pressure variation, at constant Mach).

The evolutions are of opposed senses ; this example shows well the difficulty of extending to the flight conditions, the results obtained in an

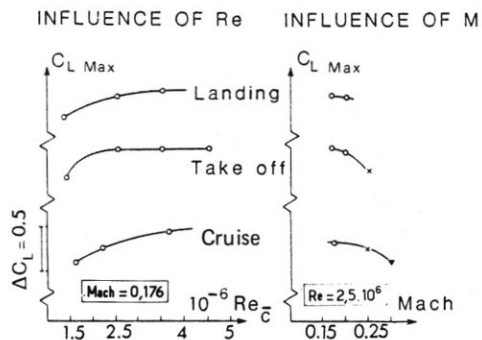


Fig. 24 – Evolution of maximum lift with Reynolds and Mach numbers.

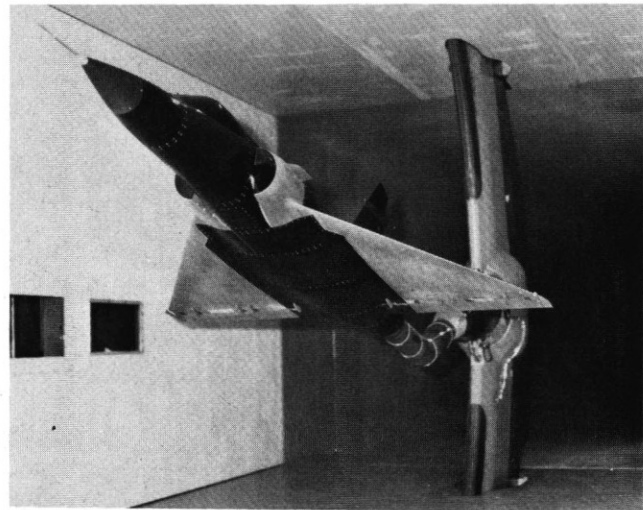


Fig. 25 – 1/4.28 scale model of Mirage 2000.

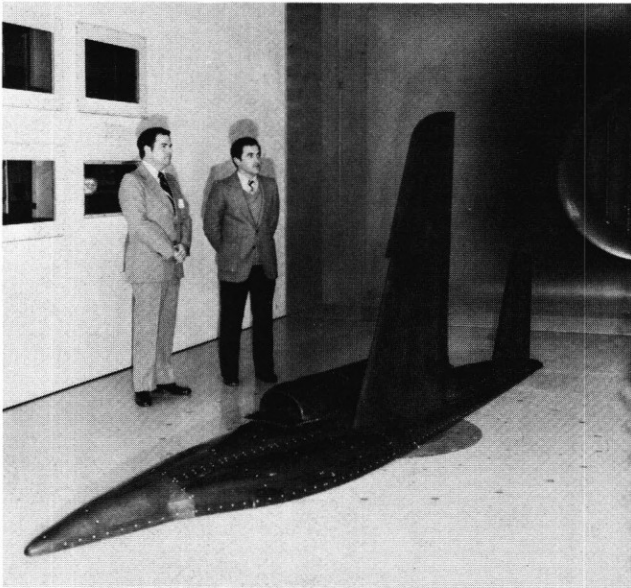


Fig. 26 – 1/2.5 scale half model of Alphajet.

#### 5.4 Variable sweep research model

A study of fundamental character is developed by the Aerodynamics Department of ONERA around a schematic wing mounted on the wall as a half model on a pivot, which enables one to change its sweep angle. The tests performed at F1 for this study made it possible to identify the relative influence of Reynolds number variations according to the configurations under test (fig. 27).

The influence of the Reynolds number on maximum lift is very important for small sweep angles, but much smaller above an angle of  $50^\circ$ .

On the contrary, for these sweep angles the onset of the vortex over this wing is very sensitive to Reynolds number.

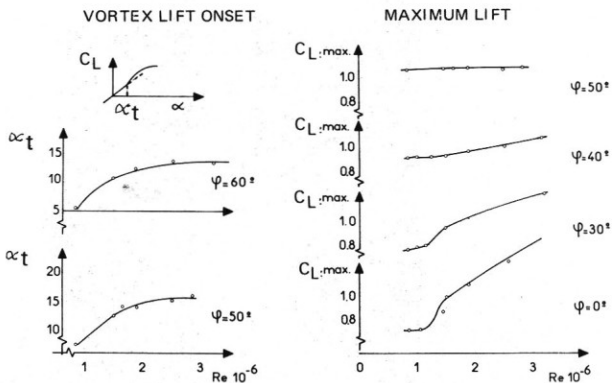


Fig. 27 – Influence of Reynolds number on a variable sweep half wing.

#### 5.5 Civil aircraft air intake

The air intake testing device, available since December 1979, has already permitted two testing campaigns, one on an A310 air intake at 1/6.25 scale, the other on an A200 air intake at 1/5 scale (fig. 28).

The results presented here are those obtained on the air intake model studied by Aérospatiale for the A200 nacelle.

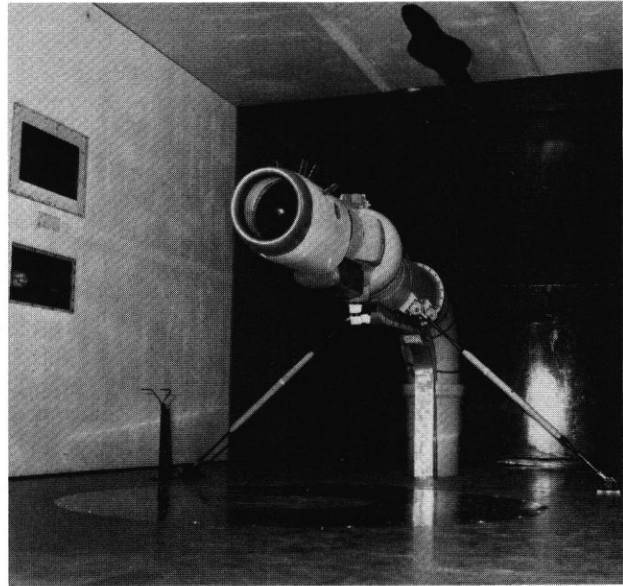


Fig. 28 – Air intake test.

Further to the determination of the air intake performance (efficiency, distortion, etc.), the tests made it possible to identify the operational limits in unusual conditions, e.g. the limit angle of attack corresponding to the stall of the upper part of the air intake in case of engine idle. Figure 29 represents the evolution of this angle of attack as a function of Reynolds number for several values of the test Mach number. At constant Mach number, the Reynolds number increase is accompanied by a noticeable increase of the separation angle of attack, that tests in an atmospheric wind tunnel would not have brought to light.

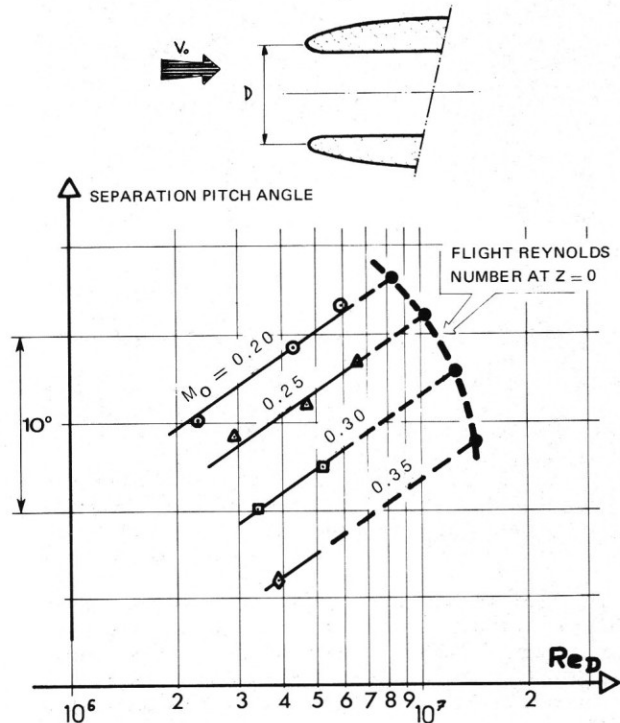


Fig. 29 – Evolution of the separation on the external upper lip of an air intake.

The large scale of the model, the stagnation pressure level and its variation at constant Mach number, the large incidence excursion permitted by the test mounting, allow one to confidently extrapolate these results to flight Reynolds numbers, at Mach 0.2 and 0.25.

### 5.6 Two-dimensional tests on profiles

Many tests have been performed on profiles for the benefit of the Aerodynamics Department by means of the new wind tunnel apparatus for two-dimensional profile tests. The tests comprise pressure readings on the profiles, the measurement of lift by integration of these pressures, and drag measurements by exploration of wake probings. Detailed probings of the flow around the profile are also ensured by various types of pressure probes and by straight or crossed hot wires.

Figure 30 is an example of plotting of velocity vectors and curves of equal pressure around the trailing edge of the profile, with a view to a detailed study of the flow in this region.

The hot wire measurements give also the unsteady components of the velocity, and the Reynolds shear stress by the average of the product of these components along the tangent and the normal to streamlines.

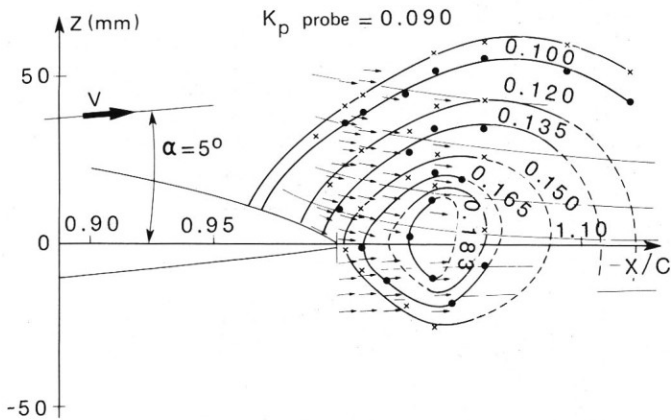
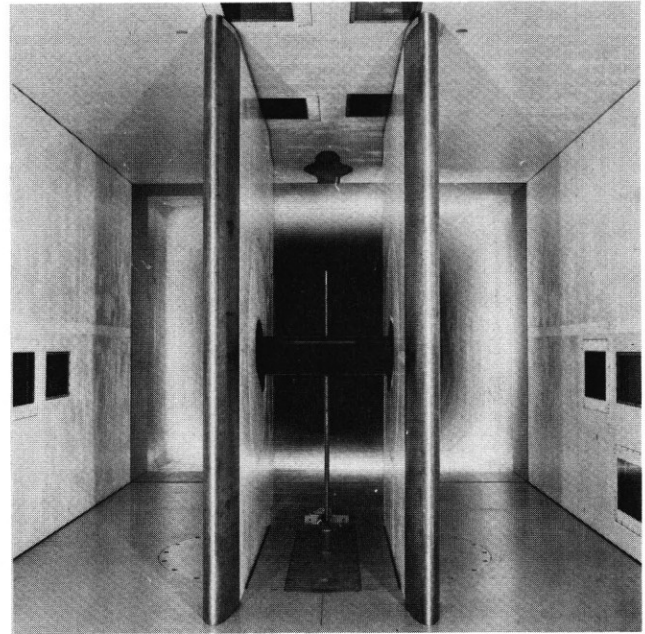


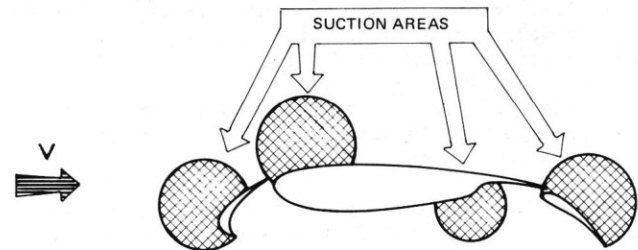
Fig. 30 - Pressure probing and flow direction around the trailing edge of a profile.

For a high lift profile placed between two flanges (fig. 31a), it is necessary to control the boundary layer by several independent zones of local suction on the flange surfaces.

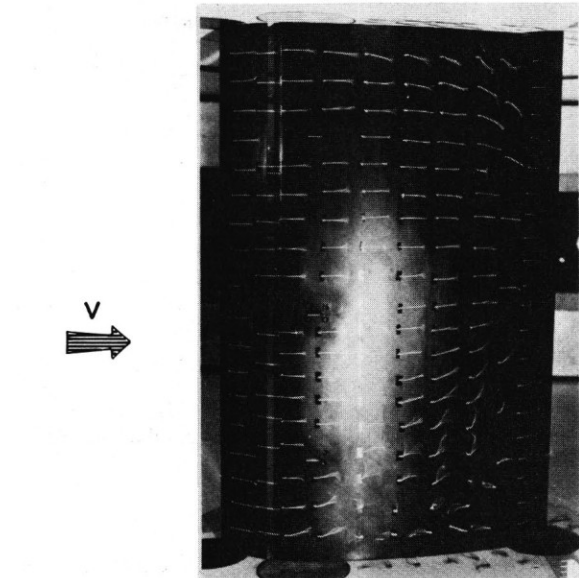
Photographs of the wall flow on the upper surface of a high lift profile, visualized by nylon tufts fixed on the profile, in the absence and in the presence of suction, show its efficiency for maintaining a two-dimensional flow (fig. 31b).

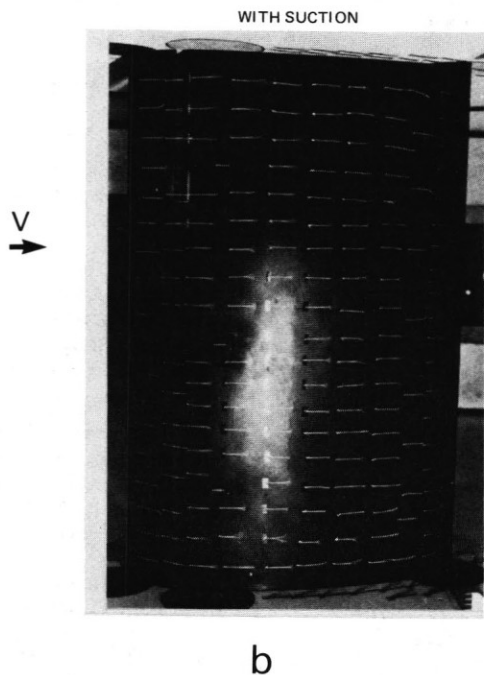


a



WITHOUT SUCTION





**b**  
 Fig. 31 – Boundary layer control of lateral flanges for a high lift profile.  
 a - Mounting between flanges.  
 b - Effect of a suction on the upper surface flow at a 12° angle of attack.

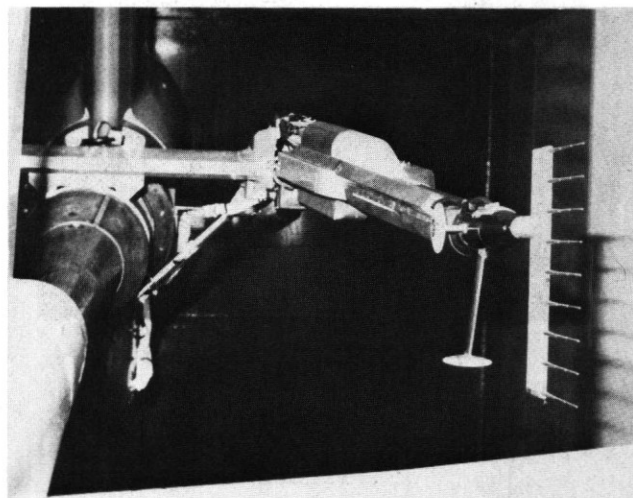
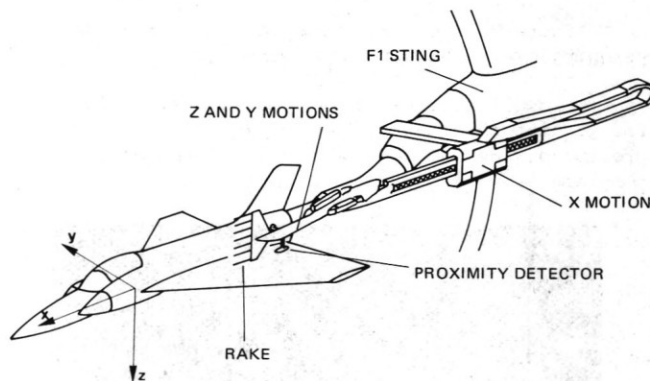


Fig. 32 – Probing device.

### 5.7 Detailed study of aerodynamic field

The number of measurements required for a wind tunnel test is ever increasing, because of the development of computing means and the new possibilities of exploitation. Tests where only global characteristics of a model are looked for are gradually replaced by tests with a fine analysis of the flow.

The number of pressure measurements on the model wall is increasing (up to 900 pressure taps on a single model, for a future test at F1) ; wall flow visualization techniques are normally used : wool or nylon tufts, sublimable coatings, viscous coatings, coloured liquids.

For the fine study of the aerodynamic field around a profile, a probing device has been designed, and a visualization technique by smoke and laser plane developed.

A probing device fixed on the sting supporting the model is made of a probe carrying arm, articulated by two parallelograms, authorizing 1-m displacements along the span  $y$ , and 0.5m along the perpendicular direction  $z$ . Translation along the axis direction  $x$  is ensured by a linear displacement mechanism with a 1.5m travel. Displacement rates are 5mm/s along  $y$  and  $z$ , and 50 mm/s along  $x$  (fig. 32).

The probing device can receive any kind of probe : single static, stagnation or clinometric probe, probe rake, rotating rake, vortex-meter, hot wire.

Figure 33 presents the result of the exploration, on the upper surface of a swept-back wing, of a plane perpendicular to the aircraft longitudinal axis, by means of a rake made of nine 5-hole clinometric probes. This plotting, obtained on-line during the test, gives in magnitude and direction the velocity projection in the probing plane.

Visualization by laser light plane and smoke also allows an exploration of the development of vortices over the whole wing, by displacement of the smoke generator and the laser plane.

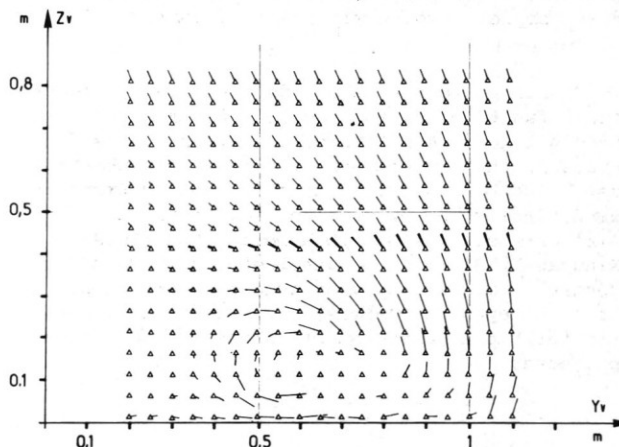


Fig. 33 – Velocity field on the upper surface of a sweptback wing.

Figure 34 shows the trace of the vortex de-veloping over a highly swept wing.

This qualitative monitoring is very useful for guiding the quantitative exploration by the probing device, so the two means are actually complementary.

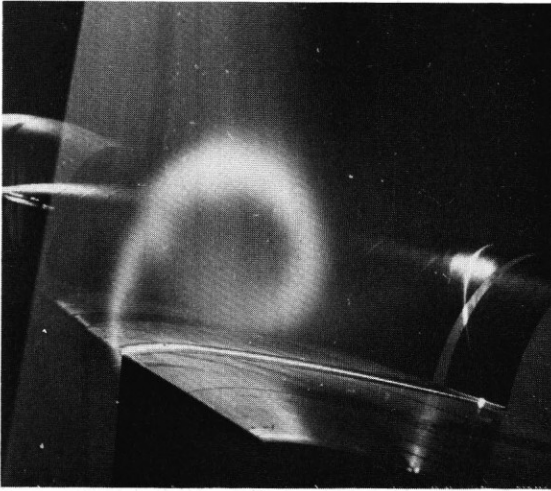


Fig. 34 - Example of visualization.

## 6. CONCLUSIONS

According to the aims that inspired its design, the F1 wind tunnel, opened to the service of aeronautical constructors and research institutes at the end of 1977, appears as a very powerful investigation tool for the experimental study of present-day aircraft.

Its aerodynamic qualities (low turbulence and very good homogeneity), its modern design (complete preparation in cells and guarantee of confidentiality), its many pieces of equipment and its performance make it possible to reach rapidly and in the best conditions, very detailed experimental results on the performance of the necessarily ever more complex aerodynamic parts of commercial or combat aircraft.

Whereas, during these first years of industrial functioning, the facility has not yet given the full measure of its capabilities, it is probable that in the near future its systematic use, side by side with the other modern European wind tunnels (5-m wind tunnel of the Royal Aircraft Establishment, DNW Deutch-Nederland-Windkanal, S1-MA wind tunnel of the ONERA Modane Centre), for the study of subsonic configurations at high Reynolds numbers, will become indispensable for the development of European aeronautical projects.

## REFERENCES

- [1] The need for large wind tunnels in Europe  
AGARD AR 60 (1972).
- [2] M. Pierre et G. Fasso - Le Centre d'essais  
aérothermodynamique de Modane-Avrieux - ONERA  
Technical Note n° 166 (1970) - also in English  
and in German.
- [3] M. Pierre - Soufflerie subsonique pressurisée  
F1 du Centre du Fauga-Mauzac de l'ONERA -  
ONERA - 11th ICAS Congress, Lisbon, September  
1978 - Provisional edition - ONERA T.P. 1978-51.
- [4] Ph. Poisson-Quinton - Some new approaches for  
wind tunnel testing through the use of compu-  
ters. First Intersociety Atlantic Aeronautical  
Conference, Williamsburg, Va. USA, March 1979 -  
Provisional Edition. ONERA T.P. 1979-24.
- [5] G Delattre - Data acquisition and processing in  
a large aerodynamic test center. AIAA paper  
n° 78-774 (1978).